

Gain spectrum measurement using the segmented contact method with an integrated optical amplifier

H. Shahid, D. T. D. Childs, M. A. Majid, K. Kennedy, R. Airey, R. A. Hogg, E. Clarke, P. Spencer, and R. Murray

Citation: [Journal of Applied Physics](#) **115**, 163105 (2014); doi: 10.1063/1.4873302

View online: <http://dx.doi.org/10.1063/1.4873302>

View Table of Contents: <http://scitation.aip.org/content/aip/journal/jap/115/16?ver=pdfcov>

Published by the [AIP Publishing](#)

Articles you may be interested in

[Semiconductor optical amplifier-based heterodyning detection for resolving optical terahertz beat-tone signals from passively mode-locked semiconductor lasers](#)

[Appl. Phys. Lett.](#) **97**, 081113 (2010); 10.1063/1.3481674

[Dispersion measurements of a 1.3 \$\mu\$ m quantum dot semiconductor optical amplifier over 120 nm of spectral bandwidth](#)

[Appl. Phys. Lett.](#) **96**, 211907 (2010); 10.1063/1.3430742

[Silicon optical amplifier based on surface-plasmon-polariton enhancement](#)

[Appl. Phys. Lett.](#) **91**, 053504 (2007); 10.1063/1.2759258

[Experimental demonstration of nonreciprocal amplified spontaneous emission in a CoFe clad semiconductor optical amplifier for use as an integrated optical isolator](#)

[Appl. Phys. Lett.](#) **85**, 3980 (2004); 10.1063/1.1811802

[Simultaneous sampling of optical pulse intensities and wavelengths by four-wave mixing in a semiconductor optical amplifier](#)

[Appl. Phys. Lett.](#) **73**, 3821 (1998); 10.1063/1.122905



Re-register for Table of Content Alerts

Create a profile.



Sign up today!



Gain spectrum measurement using the segmented contact method with an integrated optical amplifier

H. Shahid,^{1,a)} D. T. D. Childs,¹ M. A. Majid,¹ K. Kennedy,¹ R. Airey,¹ R. A. Hogg,¹ E. Clarke,² P. Spencer,² and R. Murray²

¹*Department of Electronic and Electrical Engineering, Centre for Nanoscience and Technology, The University of Sheffield, North Campus, Broad Lane, Sheffield S3 7HQ, United Kingdom*

²*Blackett Laboratory, Physics Department, Imperial College, Prince Consort Road, London SW7 2AZ, United Kingdom*

(Received 22 January 2014; accepted 14 April 2014; published online 25 April 2014)

The measurement of optical gain utilising a segmented contact and integrated optical amplifier is reported. We show that in a direct comparison of methods, the use of the integrated amplifier allows the gain spectrum to be deduced over wider spectral ranges and to lower carrier densities, as compared to the conventional segmented contact technique. © 2014 AIP Publishing LLC. [<http://dx.doi.org/10.1063/1.4873302>]

I. INTRODUCTION

The evolution of the gain spectrum of semiconductor laser materials with injected current is of critical importance in determining the static¹ and dynamic performance² of a laser, amplifier,³ or superluminescent diode.⁴ Therefore, the development of gain spectrum measurement techniques, allowing more spectral information, and over wider current density ranges, can be expected to enhance the physical understanding of laser materials.

Hakki and Paoli described a high resolution spectroscopic method applied to single mode, short length Fabry–Pérot devices.⁵ Here, net modal gain is determined from the modulation depth of the resolved peaks (constructive interference) and valleys (destructive interference) of the electroluminescence spectrum. Due to the high resolution required, accessing low carrier densities is difficult for the Hakki–Paoli method, but the method is particularly suited to high carrier densities where monitoring of the mode shift can allow a constant junction temperature to be maintained.⁶ Shaklee and Leheney⁷ described a photoluminescence measurement technique where the single pass amplified spontaneous emission was measured from the edge of the wafer, with varying optical excitation length, the gain spectrum may be deduced. Whilst this method provides a rapid feed back to epitaxy on the *potential* of the material to make a laser, the carrier/current density within the laser is unknown. Oster *et al.* developed a method which utilised contacted waveguides of different length,⁸ which allows the Shaklee and Leheney method to be carried out with known current densities. This idea was further enhanced by utilising segmented contacts upon the same waveguide by Blood *et al.*,⁹ providing the advantage that any deleterious effects due to spatial variation of the material or waveguide structure are minimised, and that a single device is optically aligned in the experimental system. In order for this method to work effectively, a spatial mode filter to eliminate unguided spontaneous emission may be needed. It was proposed and

demonstrated by Xin *et al.*,¹⁰ that the device waveguide itself could be utilised as this mode filter, further simplifying the experimental method. However, using an absorptive mode filter section results in an attenuated signal and a degradation in signal/noise, which can be expected to manifest itself in a reduced spectral coverage and reduced current range over which the gain measurement can be made. However, Xin *et al.* commented on the possible use of the mode-filter as an amplifier.¹⁰

GaAs based quantum dot (QD) devices are of interest due to their low cost, temperature insensitive threshold current density^{11,12} and their current applications in biomedical imaging,¹³ mode-locking applications,¹⁴ and optical communications.¹⁵ However, the gain spectrum in QD materials is complicated by inhomogeneous and homogeneous broadening,¹⁶ strong state-filling effects,¹⁷ and by free carrier effects.^{6,18} Quantum dot devices exhibit low transparency and threshold current densities, accompanied by modal gain saturation at low current densities, as compared to their quantum well counterparts. Low levels of spontaneous emission at these low current densities makes the measurement of gain/absorption in quantum dot laser materials a challenging task.

In this paper, we report on the use of the front sections of a QD multisection device to act as an integrated amplifier and mode filter as proposed by Xin *et al.*¹⁰ Xin *et al.* showed that using a segmented-contact device, the waveguide itself could be used as a mode filter, which is required for the removal of the unguided spontaneous emission.⁹ They also proposed that when driven into gain, this amplifier/mode filter may be beneficial in the measurement of small signals.¹⁰ Here, we compare the gain spectra obtained from the same device under operation in the standard segmented contact method,⁹ and this new method utilising an integrated amplifier under identical data acquisition conditions. We demonstrate that by using an integrated amplifier, the gain spectrum can be deduced over a wider spectral range as compared to the standard segmented contact method. Furthermore, we show that the gain spectrum can be measured (albeit over a limited spectral range) at lower current

^{a)}h.shahid@uet.edu.pk

densities when using the integrated amplifier. We go on to highlight how the measurement of the absorption/gain spectra at very low dot occupancies may allow future insight into the physics of QD laser materials.

II. DEVICE STRUCTURE

A bilayer InAs/GaAs QD laser structure¹⁹ was used for this study. The structure comprises five pairs of closely-stacked QD layers. The small separation (10 nm GaAs) between the paired layers results in preferential nucleation of QDs in the second layer above the QDs in the first (seed) layer, so that the seed layer acts as a template for QD growth in the second layer, fixing the QD density.²⁰ This allows suitable growth conditions for the second QD layer to be chosen to achieve an extension in room temperature emission from the QD ground state beyond 1300 nm, while maintaining a reasonable QD density. The small separation between the paired layers allows efficient electronic coupling between the layers so that emission occurs predominantly from the second, long-wavelength QD layer. The QD bi-layer laser material was fabricated into segmented contact devices consisting of a 10 mm long waveguide (7 μ m wide) with 1 mm long electrically isolated (>1 k Ω) contacts. Full details of the epitaxial process and the device fabrication details are given elsewhere.^{13,21} Devices were selected based upon the front four sections having identical I-V characteristics, with the assumption that this would result in identical spectral L-I characteristics.

III. EXPERIMENT

A schematic of the device drive geometries of the segmented contact device in the different measurement schemes is shown in Figure 1. Using the segmented contact method (geometry A in Fig. 1), the length of the electrically driven device is varied in order to allow the measurement of gain and absorption as a function of wavelength. In this case, the amplified spontaneous emission spectra are measured with driven section lengths of L and 2L (where L = 1 mm for these devices) at a given current density. The comparison of

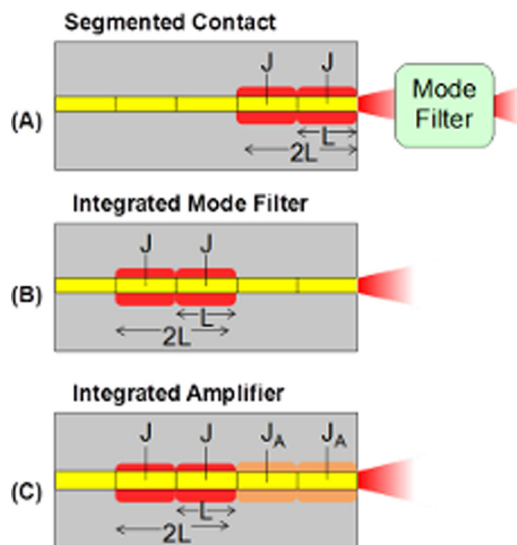


FIG. 1. Schematic of the different device drive geometries employed.

the spectra at each wavelength indicates the presence of gain (or loss) at that particular wavelength which can be calculated using the following equation:⁹

$$\text{Net Modal Gain} = \frac{1}{L} \ln \left(\frac{I_{2L}}{I_L} - 1 \right). \quad (1)$$

Introducing an integrated mode filter may be achieved by introducing un-pumped sections of the waveguide at the output of the device in geometry B (Fig. 1). The electrically driven sections are operated in exactly the same manner as in the segmented contact method, and the net modal gain can again be determined by the relationship given by Eq. (1).

An integrated amplifier is obtained by driving the same mode filter sections of the device into gain over the spectral region of interest. This is shown schematically in geometry C in Figure 1, where the front sections acts as a combined amplifier/mode filter. In order to deduce the gain spectrum, initially the emission spectrum with only the amplifier/mode filter is measured, in our case, this is with the front two sections at a current density of J_A . This intensity, I_A (guided and unguided spontaneous emission), is subtracted from the intensities I_L (driving a single contact at a given current density) and I_{2L} (driving two contacts at a given current density). The net modal gain in this case can be deduced using Eq. (2),¹⁰ and the unamplified spontaneous emission spectra were determined by using Eq. (3).¹⁰

$$\text{Net Modal Gain} = G = \frac{1}{L} \ln \left(\left(\frac{I_{2L} - I_A}{I_L - I_A} \right) - 1 \right), \quad (2)$$

$$\text{Spontaneous Emission} = G \left(\frac{(I_{2L} - I_L)}{(e^{GL} - 1) e^{GL}} \right). \quad (3)$$

The measurement system is shown schematically in Figure 2. It is important to note that for a fair comparison of the different methods, an external mode filter is not employed for the segmented contact method. This ensures that the light collection efficiency is constant for all the cases. All the acquisition parameters (spectral resolution, sensitivity, integration times, and coupling efficiency) were constant, and the same device was used for all these comparative measurements. The Optical Spectrum Analyser sensitivity was set just above the noise floor to access the lowest possible current density emission spectra.

IV. RESULTS AND DISCUSSION

Generally with these methods, the gain/absorption spectrum can only be determined at wavelengths at which

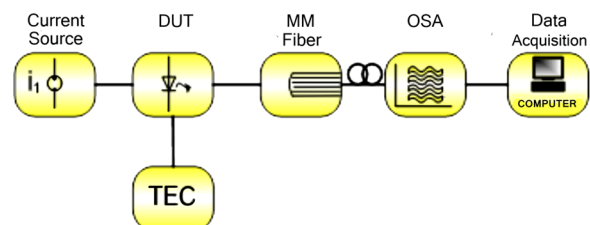


FIG. 2. Experimental setup for three gain measurement schemes.

spontaneous emission occurs and is above the noise floor of the measurement system. Figure 3(a) plots the spontaneous emission spectrum at 14 A/cm^2 at which current density the material is operating in loss over the whole spectral region. It is therefore expected that depending upon the value of the absorption and details of spectral acquisition, the gain spectrum may not be obtained where there is limited emission, such as at shorter wavelengths, i.e., $< \sim 1275 \text{ nm}$ where spontaneous emission is weak and may be lost in the noise floor of the detection system. Figure 3(b) plots the gain spectrum obtained via the segmented contact method obtained at a current density of 1.42 kA/cm^2 . Here, positive net modal gain is obtained from $\sim 1175 \text{ nm}$ to 1375 nm .

The optical power as a function of current density is plotted for two device geometries in Figure 4(a). The schematic legend shows the current drive geometries for the device. In the case of the integrated amplifier, the optical power obtained when $J_A = 1.42 \text{ kA/cm}^2$, and $J = 0$ is subtracted from the power, to show the power just from the gain measurement sections. The results show an increase in optical power obtained in the case of integrated amplifier for each current density step in comparison to the segmented contact measurement. Figure 4(b) plots the optical gain (dB) as a function of current density obtained using integrated amplifier technique. It is observed that an approximately 3 dB gain/amplification is realized in the optical signal at each current density by using integrated amplifier technique. The observed ripple is attributable to unguided spontaneous emission which is later on removed via integrated amplifier method.

Comparison of the gain spectra deduced using the three measurement schemes (described in Fig. 1) is shown in

Fig. 5. Here, the gain is determined at a current density, J , of 350 A/cm^2 with an amplifier current density, J_A , of 350 A/cm^2 for the integrated amplifier method. Towards long wavelengths all three techniques show essentially identical results with regard to the spectral shape and magnitude of the gain from the ensemble of quantum dot ground states. At shorter wavelengths, the methods utilizing the integrated mode filter and integrated amplifier give essentially identical results. The gain spectrum may not be obtained for shorter wavelengths with these data acquisition parameters utilizing the integrated mode filter method due to attenuation of the emission (the integrated mode filter is operating in loss) resulting in the signal being indistinguishable from the noise floor at wavelengths less than 1250 nm .

For both techniques that utilize the mode filter, towards shorter wavelengths, a slightly different gain spectrum is obtained in comparison with the segmented contact method. The difference suggests either the presence of unguided spontaneous emission in configuration A or it may be due to the spatial inhomogeneity of the sample. However, similar measurements for different materials where the length of the contact was varied have shown similar results, suggesting that this difference is due to unguided spontaneous emission. The observation of a change in the excited state gain but not in ground state gain between the different spectra in Figure 5 is unlikely to be explained by spatial inhomogeneity of the sample (varying, for example, the QD areal density), as it would affect both the ground state and excited state. We cannot rule out a spatial variation in carrier lifetime or in variations in the width or depth of the etched waveguide giving rise to this small difference.

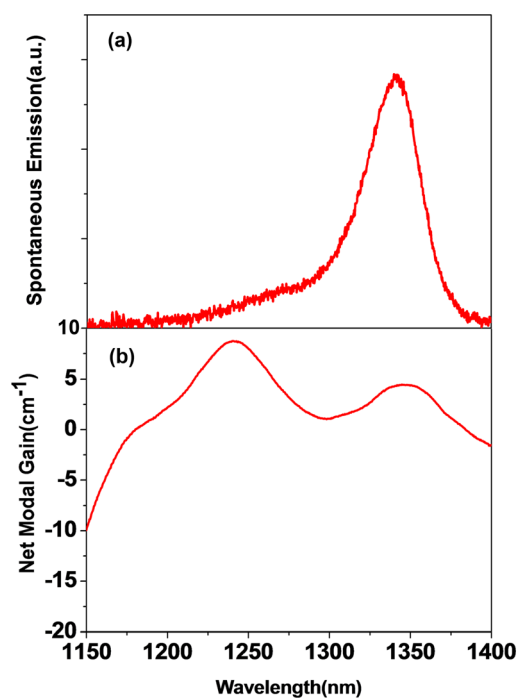


FIG. 3. (a) Spontaneous emission spectrum at 14 A/cm^2 by pumping a section of length L . (b) Net modal gain spectrum at 1.42 kA/cm^2 obtained from the amplifier section as a function of wavelength measured by the segmented contact method.

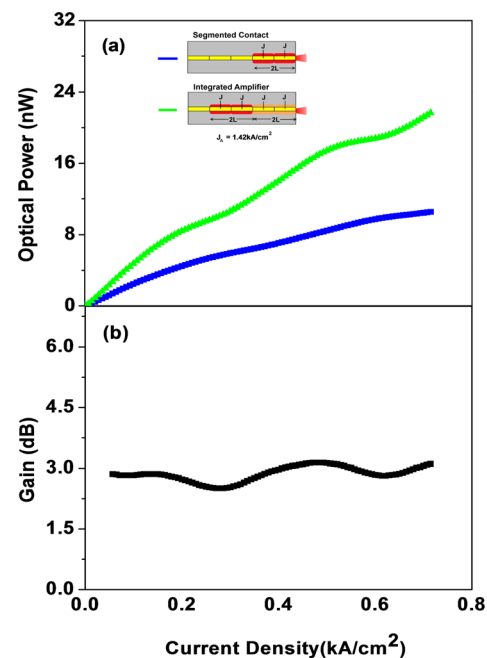


FIG. 4. (a) Schematic of the different device drive geometries employed. L-J (optical power vs. current density) characteristics of a bilayer multisection device; blue is without an integrated amplifier, and green is obtained while maintaining a current density of 1.42 kA/cm^2 in an integrated amplifier section under continuous wave mode of operation. (b) Optical gain (dB) vs. current density showing $\sim 3 \text{ dB}$ gain as deduced from Fig. 4(a).

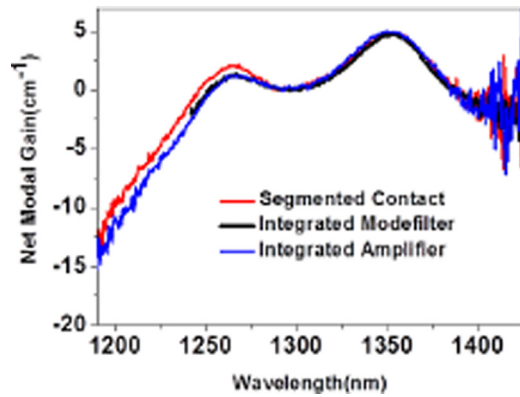


FIG. 5. Net modal gain spectra as a function of wavelength for $J = 350 \text{ A/cm}^2$ and $J_A = 350 \text{ A/cm}^2$ utilizing schemes A, B, and C.

Figure 6(a) plots the gain spectra as a function of current density for the segmented contact method and in Fig. 6(b) for the integrated amplifier method with an amplifier current density $J_A = 1.42 \text{ kAcm}^{-2}$. For these plots, the data are manually inspected, and only the data where the signal can be discriminated from the noise floor are plotted, resulting in the truncation of the gain curves for low drive current densities. Under identical data acquisition conditions, at a given current density, the gain spectrum is obtained over a wider spectral range for the integrated amplifier. The difference in spectral width over which gain is measured becomes smaller as the current density in the sections being measured is increased, where the sections under test are no longer in loss, but are themselves operating in gain. For low current

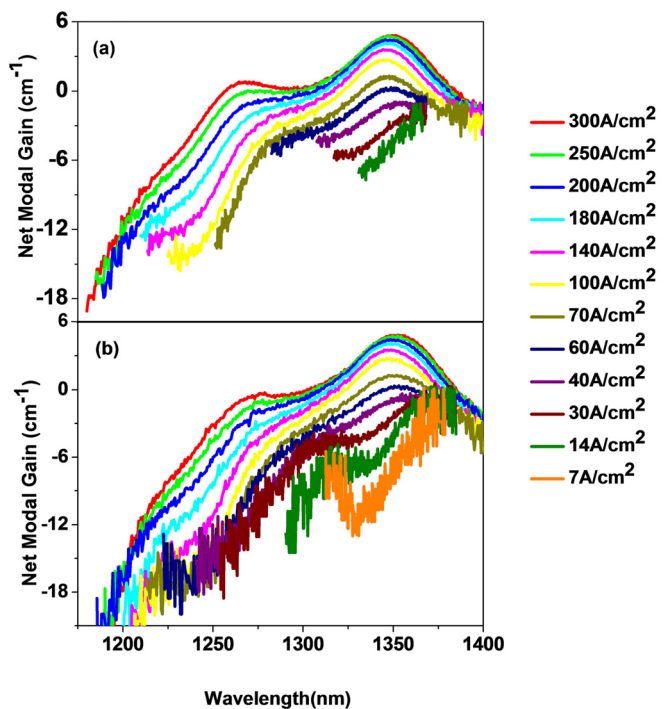


FIG. 6. Net modal gain spectra as a function of wavelength for (a) a current density range of 14 A/cm^2 – 300 A/cm^2 utilizing the segmented contact method and (b) 7 A/cm^2 – 300 A/cm^2 utilizing the integrated amplifier method.

densities, the difference is clearer, in terms of enhanced spectral coverage of the measurement and with some current densities only being accessed through the use of the integrated amplifier. We note that the signal:noise ratio of the deduced gain spectrum varies in the two measurement techniques. For comparatively high current densities, the integrated amplifier method introduces higher levels of noise (c.f. spectra at 300 Acm^{-2}), whilst at low current densities over the same spectral region, the integrated amplifier method results in lower noise levels (c.f. spectra at 14 Acm^{-2}). At low current densities, the amplification of the signal assists in being able to distinguish between the noise floor and the signal, whilst at higher J , the amplifier introduces additional shot noise.

It should be noted that for the segmented contact method, the external mode filter was omitted. The introduction of this component will introduce additional loss reducing the signal to noise ratio, which is in turn expected to further enhance the benefits of using an integrated amplifier. We also note that these measurements are for the case where sensitivity is fixed. Further work is required to determine if the method has application in systems where the sensitivity can be varied.

In the following, we briefly comment upon a comparison of spontaneous emission and gain spectra for this QD material made possible by using this measurement method. Figure 7(a) plots the modal gain spectrum as a function of current density derived from Figure 6(b) (obtained through the integrated amplifier method), including an internal loss, $\alpha_i = 2 \text{ cm}^{-1}$. A blue-shift in the gain peak is observed with increasing current density, which has been attributed to carrier thermalisation and state-filling within the ensemble of

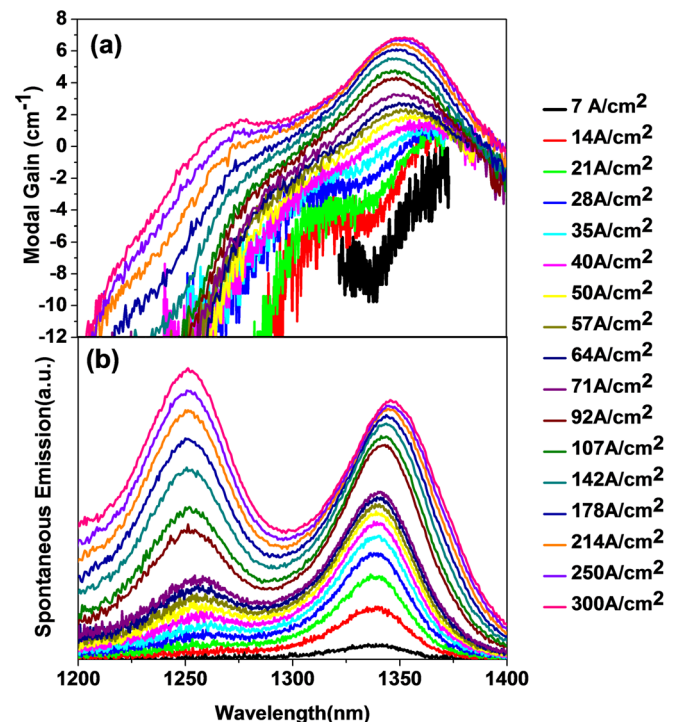


FIG. 7. (a) Modal gain and (b) spontaneous emission spectra obtained by integrated amplifier method.

QDs.²² Figure 7(b) plots the spontaneous emission spectrum over the same current densities, obtained using the same method.⁹ By comparing the magnitude of the electroluminescence when the QD ground-state is saturated, and that of the lowest current density (7 A cm^{-2}), we estimate that the average dot occupancy is ~ 0.04 electron-hole pairs per QD.

Due to the low dot occupancy which can be accessed using the integrated amplifier, the measurement of the gain/absorption in conditions when the QDs are essentially empty, yet under identical bias conditions is made possible. In Fig. 7(a), a modal absorption of $9 \pm 1 \text{ cm}^{-1}$ is measured for the ground state. The saturated modal gain of the ground state (at $\sim 300 \text{ A cm}^{-2}$) is $7 \pm 1 \text{ cm}^{-1}$. These values are very similar, which contrasts previous reports where absorption spectra and gain spectra were compared under different bias conditions,^{9,23} where very different values for absorption and saturated gain were compared. Measurements of the linewidth of the ground-state saturated gain and the absorption at the lowest current density give values of $\sim 50 \text{ nm}$ for gain (34 meV), whilst the absorption peak has a linewidth of $\sim 35 \text{ nm}$ (28 meV). We note that the product of linewidth and absorption/gain is very similar in both cases ($34 \times 7 = 238 \text{ meV cm}^{-1}$, $28 \times 9 = 252 \text{ meV cm}^{-1}$). The difference in the both line-width and absorption/saturated gain is attributed to the different possible carrier occupancies of the filled quantum dot leading to an additional broadening mechanism (due to different magnitudes of the free carrier shift of the band-gap) which reduces the peak gain,⁶ as compared to the peak absorption at these biases.

Figure 7(b) shows that as expected, at low current density, the spontaneous emission and absorption peak are observed to be coincident ($1338 \text{ nm}/0.93 \text{ eV}$). The measurement of the absorption peak at the positive biases where light emission occurs is typically not reported. However, at high current density, the spontaneous emission and peak in gain do not coincide, with the gain peak being $\sim 4 \text{ meV}$ smaller in energy. Self-heating effects are identical in both cases as these spectra are deduced from the same measurement. The observation that the spontaneous emission does not significantly shift in peak position from low occupancies (0.04 e-h pairs per QD) to ground state saturation appears at odds with the blue shift of the gain peak with increasing current density. If a thermalised carrier population is present, then a blue-shift of the ground-state emission is also expected. A possible explanation of the results is that there is a random carrier population of the QDs, along with strong many-body effects that modify the gain and spontaneous emission spectra. A random carrier population would explain the essentially identical QD ground-state EL spectra. Free carrier effects, which shift the emission and gain of the QDs with high electron-hole pair occupancy, may then give rise to the observed blue-shift of the gain peak. In order to confirm this tentative proposal, more sensitive measurements are required. The analysis and theoretical modeling of EL and gain/absorption spectra where the absorption peak is fully resolved (and are obtained at even lower dot occupancies), over a range of temperatures, are required.

V. CONCLUSIONS

In this paper, we have demonstrated the use of an integrated amplifier and mode-filter in the measurement of single-pass gain in semiconductor laser material. A direct comparison of three segmented contact gain measurement techniques has shown that for low current densities where the material operates in loss, the gain can be measured over a wider spectral region utilising the integrated amplifier. Furthermore, the measurement of the gain spectrum at very low current densities is made possible. We then discuss how this method enables the analysis of gain/absorption and EL spectra of QDs at very low dot occupancies, which may, in future, cast light on fundamental physical processes.

ACKNOWLEDGMENTS

This work was funded under EPSRC Grant No. EP/FO3427X/1. H. Shahid gratefully acknowledges support from the University of Engineering and Technology (K.S.K. campus), Lahore, Punjab, Pakistan.

- ¹P. W. A. Mc Ilroy, A. Kurobe, and Y. Uematsu, *IEEE J. Quantum Electron.* **21**, 1958 (1985).
- ²Y. Arakawa and A. Yariv, *IEEE J. Quantum Electron.* **22**, 1887 (1986).
- ³M. J. Connelly, *IEEE J. Quantum Electron.* **37**, 439 (2001).
- ⁴G. A. Alphonse, G. B. Gilbert, M. G. Harvey, and M. Ettenberg, *IEEE J. Quantum Electron.* **24**, 2454 (1988).
- ⁵B. W. Hakki and T. L. Paoli, *J. Appl. Phys.* **46**, 1299 (1975).
- ⁶H. Shahid, D. T. D. Childs, B. J. Stevens, and R. A. Hogg, *Appl. Phys. Lett.* **99**, 061104 (2011).
- ⁷K. L. Shaklee and R. F. Leheny, *Appl. Phys. Lett.* **46**, 475 (1971).
- ⁸A. Oster, G. Erbert, and H. Wenzel, *Electron. Lett.* **33**, 864 (1997).
- ⁹P. Blood, G. M. Lewis, P. M. Smowton, H. D. Summers, J. D. Thomson, and J. Lutti, *IEEE J. Sel. Top. Quantum Electron.* **9**, 1275 (2003).
- ¹⁰Y. C. Xin, Y. Li, A. Martinez, T. J. Rotter, H. Su, L. Zhang, A. L. Gray, S. Luong, K. Sun, Z. Zou, J. Zilko, P. M. Varangis, and L. F. Lester, *IEEE J. Quantum Electron.* **42**, 725 (2006).
- ¹¹K. Otsubo, N. Hatori, M. Ishida, S. Okumura, T. Akiyama, Y. Nakata, H. Ebe, M. Sugawara, and Y. Arakawa, *Jpn. J. Appl. Phys.* **43**, 1124 (2004).
- ¹²S. Fathpour, Z. Mi, P. Bhattacharya, A. Kovsh, S. Mikhlin, I. Krestnikov, A. Kozhukhov, and N. Ledentsov, *Appl. Phys. Lett.* **85**, 5164 (2004).
- ¹³P. D. L. Greenwood, D. T. D. Childs, K. Kennedy, K. M. Groom, M. Hugues, M. Hopkinson, R. A. Hogg, N. Krstajić, L. E. Smith, S. J. Matcher, M. Bonesi, S. MacNeil, and R. Smallwood, *IEEE J. Sel. Top. Quantum Electron.* **16**, 1015 (2010).
- ¹⁴E. U. Rafailov, M. A. Cataluna, and W. Sibbett, *Nat. Photonics* **1**, 395 (2007).
- ¹⁵K. Takada, M. Ishida, Y. Nakata, T. Yamamoto, M. Yamaguchi, K. Nishi, M. Sugawara, and Y. Arakawa, *IEEE Asia Commun. Photon. Conf. Exh. 2010*, 577.
- ¹⁶M. Sugawara, K. Mukai, Y. Nakata, and H. Ishikawa, *Phys. Rev. B* **61**, 7595 (2000).
- ¹⁷A. Markus, J. X. Chen, O. Gauthier-Lafaye, J.-G. Provost, C. Paranthoën, and A. Fiore, *IEEE J. Sel. Top. Quantum Electron.* **9**, 1308 (2003).
- ¹⁸I. O'Driscoll, M. Hutchings, P. M. Smowton, and P. Blood, *Appl. Phys. Lett.* **97**, 141102 (2010).
- ¹⁹E. C. Le Ru, P. Howe, T. S. Jones, and R. Murray, *Phys. Rev. B* **67**, 165303 (2003).
- ²⁰P. Howe, E. C. Le Ru, E. Clarke, B. Abbey, R. Murray, and T. S. Jones, *J. Appl. Phys.* **95**, 2998 (2004).
- ²¹M. A. Majid, D. T. D. Childs, H. Shahid, S. C. Chen, K. Kennedy, R. J. Airey, R. A. Hogg, E. Clarke, P. Spencer, and R. Murray, *Jpn. J. Appl. Phys., Part 2* **50**, 04DG10-1 (2011).
- ²²R. Heitz, F. Guffarth, I. Mukhametzhanov, M. Grundmann, A. Madhukar, and D. Bimberg, *Phys. Rev. B* **62**, 16881 (2000).
- ²³I. C. Sandall, C. L. Walker, P. M. Smowton, D. J. Mowbray, and H. Y. Liu, *IEE Proc.-J: Optoelectron.* **153**, 316 (2006).